LBL-11038
Preprint

Lawrence Berkeley Laboratory
UNIVERSITY OF CALIFORNIA

Materials & Molecular
Research Division

Submitted to The Journal of Chemical Physics

MODEL STUDIES OF MODE-SPECIFICITY IN UNIMOLECULAR REACTION DYNAMICS

Boyd A. Waite and William H. Miller

June 1980

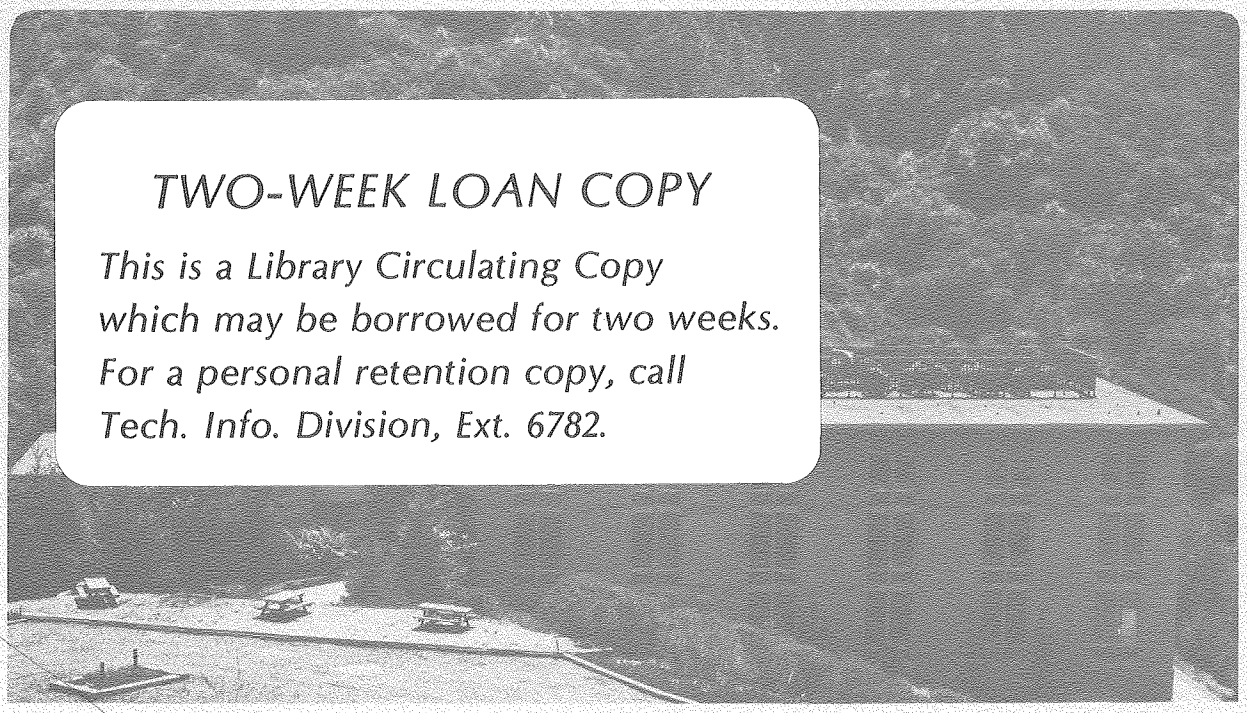

Prepared for the U.S. Department of Energy under Contract W-7405-ENG-48

DISCLAIMER

LBL-11038

MODEL STUDIES OF MODE-SPECIFICITY IN UNIMOLECULAR REACTION DYNAMICS*

By

Boyd A. Waite and William H. Miller

Department of Chemistry, Materials and Molecular Research Division
Lawrence Berkeley Laboratory, University of California,
Berkeley, California 94720

*Preliminary results of this work were presented at the Second West Coast Theoretical Chemistry Symposium, Pasadena, April 9-11, 1980.

Abstract

Essentially exact quantum mechanical calculations are carried out to determine the energies and lifetimes of the quasi-bound states for a system of two (non-linearly) coupled oscillators (one of which is harmonic, the other being able to dissociate). For weak coupling the system displays mode-specificity, i.e., the unimolecular rate constants are not a monotonic function of the total energy, but increased coupling and frequency degeneracy tends to destroy mode-specificity. A somewhat surprising result is that for a given coupling the degree of mode-specificity is roughly independent of the energy, in marked contrast to the fact that there is an energetic threshold for the onset of "stochastic trajectories" of the corresponding classical system; i.e., there seems to be no relation between statistical/mode-specific behavior of the unimolecular rate constants and stochastic/regular classical trajectories. In order to be able to treat more physically relevant models--i.e., those with more than two degrees of freedom--a semiclassical model is constructed and seen to be able to reproduce the accurate quantum mechanical rates reasonably well.

I. Introduction

The possibility of mode-specific chemistry is one of the interesting questions that has been spurred in recent years by the advent of lasers.[1] If a molecule is excited in a specific way, as is possible with a laser, and if attention is restricted to isolated, collisionless molecular systems, then the basic question is whether or not unimolecular chemistry will occur before intramolecular relaxation processes destroy the specificity of the excitation. Stated another way, one asks if the rate of reaction and/or other characteristics of the reaction, such as the distribution of products, depends not just on the amount of excitation energy but on the specific way this energy is put into the molecule, i.e., on which modes are excited.

For one extreme class of molecules, Van der Waals complexes in a molecular beam, mode-specificity is obvious. For a given amount of vibrational energy in $I_2 \cdots He$, for example,[2] no one is surprised that the rate of decomposition depends on whether the energy is initially in vibration of I_2 or in the Van der Waals bond. For more normal molecules, however, it has commonly been assumed that mode-specific effects are unimportant,[3] although several recent experimental studies claim to observe them.[4]

Recent theoretical work[5] related to mode-specific chemistry has taken two directions, one addressing itself to the abstract question of ergodicity (classical or quantum mechamical) of the intramolecular dynamics, and the other dealing more directly with the dynamics of unimolecular reactions. The present paper is of the latter category, and our current thinking is that this is in general a more fruitful

way to address the question. Whether the intramolecular dynamics is formally ergodic or not in an infinite time limit does not seem as relevant to mode-specificity as does the rate of intramolecular energy transfer compared to the rate of the chemistry of interest. This point can be illustrated by considering an elementary 2-state model of a unimolecular reaction: The rate of intramolecular transfer between states 1 and 2 is k_{in}, and states 1 and 2 react at rates k_1 and k_2, respectively; the kinetic scheme is

$$1 \underset{k_{in}}{\overset{k_{in}}{\rightleftharpoons}} 2 \qquad (1.1a)$$

$$1 \xrightarrow{k_1} \text{products}$$

$$2 \xrightarrow{k_2} \text{products} \quad . \qquad (1.1b)$$

The intrinsic reaction rates (the eigenvalues of the master equation) are easily found to be

$$\text{rate} = \tfrac{1}{2}(k_1+k_2) \pm \frac{(\frac{k_1-k_2}{2})^2}{k_{in} + \sqrt{k_{in}^2 + (\frac{k_1-k_2}{2})^2}} \quad . \qquad (1.2)$$

This system is ergodic by construction--i.e., it hops back and forth between states 1 and 2 with equal rates, and thus on the average spends the same amount of time in each--but reacts at the statistical rate, $\frac{1}{2}(k_1+k_2)$, only in the limit $k_{in} >> |\frac{k_1-k_2}{2}|$. In the opposite limit the system is mode-specific--i.e., the rate given by Eq. (1.2) is k_1 or

k_2--even though the intramolecular dynamics is ergodic.

The strategy in this paper is to investigate a simple model for unimolecular reaction, namely two coupled oscillators, one of which can dissociate. The object is to calculate the unimolecular reaction rates, varying relevant parameters of the potential energy surface to see which are most important in distinguishing between mode-specific and statistical behavior. There have been a number of studies of unimolecular decomposition of two-oscillator systems,[6] but one of the problems with them has been that two degrees of freedom are so few that it is actually difficult ever to observe statistical behavior; i.e., with only two degrees of freedom the molecule decomposes too fast for any amount of coupling between the oscillators to yield the purely statistical limit. In an attempt to circumvent this shortcoming of two-oscillator models we have chosen the dissociative oscillator to have a potential barrier to dissociation so that the reaction must proceed by tunneling. By varying the size of $\hbar$ one can thus slow down or speed up the rate of dissociation (tunneling) without significantly affecting the intramolecular vibrational dynamics; to the extent that the intramolecular dynamics is described well by classical mechanics, varying $\hbar$ does not change it at all.

The particular model we study is described in Section II, as well as a more definite meaning of what we interpret as mode specificity. Section III then describes the method by which the essentially exact quantum mechanical rates were calculated and discusses the results, i.e., the influence of various aspects of the potential surface, resonance effects, etc., on mode-specificity of the reaction rates.

Some of these results are the expected ones--e.g., increased coupling and degeneracy between the frequencies of the two modes tends to destroy mode-specificity in the unimolecular rate constants--but others are somewhat surprising: the degree of mode-specificity in the rate constants is roughly independent of energy, in contrast to the energy threshold[7] which is necessary for stochastic-like trajectories of the corresponding classical system. Since rigorous quantum mechanical calculations will be impractical for systems with many degrees of freedom, a semiclassical model is described and applied in Section IV; the results of it are in reasonably good agreement with the exact quantum mechanical results. Section V summarizes the conclusions of the study and concludes with a brief discussion of some additional aspects if preparation of the excited states is not direct; e.g., in the photodissociation of formaldehyde[8] the initial excitation is to a bound state of S_1, the first excited singlet state, followed by a non-adiabatic transition back to the vibrationally excited ground electronic state S_0, and then dissociation:

$$H_2CO + h\nu \rightarrow H_2CO^*(S_1) \tag{1.3a}$$

$$H_2CO^*(S_1) \rightarrow H_2CO^{\ddagger}(S_0) \rightarrow H_2 + CO \quad . \tag{1.3b}$$

II. The Model

The Hamiltonian for the two-oscillator system we consider is

$$H = \frac{p_x^2}{2m} + \frac{p_y^2}{2m} + V_1(x) + \frac{1}{2} m\omega_y^2 y^2 + V_c(x,y) \quad , \qquad (2.1)$$

where $V_1(x)$ is a potential function as shown in Figure 1, and V_c is the interaction which couples the two oscillators. This system has only metastable, or quasi-bound vibrational states, which are characterized by complex energies $E_r - i\Gamma/2$. The real part of the complex energy, E_r, is the energy of the metastable state, and the imaginary part is related to its lifetime τ and unimolecular decay rate k by

$$k \equiv \tau^{-1} = \Gamma/\hbar \quad . \qquad (2.2)$$

The goal of a theoretical treatment of this system is to determine the complex energies for all the quasi-bound states, and they then provide the energies and lifetimes (i.e., decay rates) of all the metastable states of the system.

It is illustrative to consider first the uncoupled case, i.e., $V_c \equiv 0$ in Eq. (2.1). The complex energies are then characterized by a quantum number for each oscillator and are additive,

$$E_{n_x,n_y} = (\varepsilon_{n_x} - i\Gamma_{n_x}/2) + \varepsilon_{n_y} \quad ,$$

where it has been noted that in this uncoupled limit only the energy of the x-mode is complex. The energy E and rate constant k for the

quasi-bound state with quantum numbers (n_x, n_y) are thus

$$E_{n_x,n_y} = \varepsilon_{n_x} + \varepsilon_{n_y} \tag{2.3a}$$

$$k_{n_x,n_y} = \Gamma_{n_x}/\hbar \quad . \tag{2.3b}$$

This is the extreme limit of mode-specificity: The rate depends only on the quantum number (and thus the energy) of the x-mode. This mode-specific or non-statistical character is seen more dramatically in a plot of the rate constant k versus total energy E, as in Figure 2: For a statistical, or RRKM-like system,[9] k should be a smooth monotonically increasing function of the total energy E, and the present uncoupled system depicted in Figure 2 is clearly the opposite extreme.

Suppose, however, one considers the limit of many closely spaced energy levels and computes the <u>average</u> rate constant at energy E,

$$k(E) \equiv \frac{\sum_{n_x,n_y} k_{n_x,n_y}\, \delta(E-E_{n_x,n_y})}{\sum_{n_x,n_y} \delta(E-E_{n_x,n_y})} \quad , \tag{2.4}$$

where in actuality the δ-functions should be broadened enough so that at least several quasibound states have energies within their width about E. With the separable approximation in Eq. (2.3), plus the semiclassical approximation[10] to Γ_{n_x},

$$\Gamma_{n_x} \simeq P(\varepsilon_{n_x}) \frac{\partial \varepsilon_{n_x}}{\partial n_x}/2\pi \quad , \tag{2.5}$$

where P is the one-dimensional tunneling probability for the x-mode, and the continuum limit

$$\sum_{n_x} \rightarrow \int dn_x \quad , \tag{2.6}$$

it is a simple calculation to convert Eq. (2.4) into

$$k(E) = [2\pi\hbar\rho(E)]^{-1} \sum_{n_y} P(E - \varepsilon_{n_y}) \quad , \tag{2.7}$$

which is recognized as the RRKM rate expression including tunneling.[11] ($\rho(E)$, the denominator of Eq. (2.4), is the density of quasibound states.) Thus the <u>average</u> rate constant at total energy E is, essentially by definition, the RRKM statistical rate even if there is no coupling between the modes. k(E) is, of course, a smooth monotonically increasing function of E. Even if there is coupling between the modes, it is still possible of course to define the average rate k(E) for a given total energy E by averaging the individual rate constants over some energy interval.

The fundamental question with regard to mode-specific chemistry is, when coupling between the modes is introduced, do all the points in Figure 2 move and fall along a <u>single</u> smooth monotonically increasing curve ($\equiv$ k(E)); i.e., does the unimolecular decay rate of each <u>individual</u> quasi-bound state depend only on its total energy (and thus equal its average value at that energy, the RRKM statistical rate). To investigate the extent to which this does or does not happen is the purpose of the numerical calculations described below.

The particular functional forms used for the potentials in the Hamiltonian of Eq. (2.1) are

$$V_1(x) = \frac{1}{2} m\omega_x^2 x^2 \, e^{-x^2} \tag{2.8a}$$

$$V_c(x,y) = x^2 e^{-x^2} \left[V_2 y - \eta \frac{m\omega_y^2}{2} y^2\right] \quad . \tag{2.8b}$$

The potential energy is harmonic near the bottom of the well with frequencies ω_x and ω_y, and through cubic anharmonicities it is identical to the well-studied Barbanis potential.[12] It is of interest to see if any of the classical ergodic features[7] of the system are relevant to mode-specificity of the unimolecular rate constants. The coupling interaction in Eq. (2.8b) has two terms: the η coupling serves to dilute the transverse frequency in the saddle point region, i.e., to widen the valley leading to products, and the V_2 coupling introduces curvature in the reaction path, the path of steepest descent down from the saddle points. These are the two kinds of coupling[13] present in real systems, and one would like to identify which is most closely associated with mode-specific/statistical behavior.

III. Quantum Mechanical Calculations

The complex energies which characterize quasibound states are defined rigorously as the poles of the analytically continued Green's function, or equivalently, of the S-matrix.[14] In a scattering experiment they appear as resonances, with the width of a resonance being the imaginary part of the complex energy. The complex energies can also be defined as the eigenvalues of the Schrödinger equation with purely outgoing wave boundary conditions.[15]

Within the last few years several new methods have appeared for calculating these complex energy eigenvalues by variational methods quite similar to those used for ordinary bound states. The Siegert eigenvalue approach[15,16] applies the outgoing wave boundary condition directly, but the complex scaling method,[17] which is closely related to it, is more convenient for our present purposes since it permits the calculations of many complex eigenvalues simultaneously.

The complex scaling method[17] makes the following transformation of the Hamiltonian by scaling the coordinates $\underset{\sim}{x}$ by

$$\underset{\sim}{x} \rightarrow \underset{\sim}{x}\, e^{i\theta}$$

so that

$$H(\underset{\sim}{x}) \rightarrow H(\underset{\sim}{x}\, e^{i\theta}) \equiv H_\theta \quad ; \tag{3.1}$$

the kinetic energy operator scales as $\frac{d^2}{dx^2} \rightarrow e^{-2i\theta} \frac{d^2}{dx^2}$. Such a transformation has the following effects on the spectrum of energy

eigenvalues: (1) bound state eigenvalues (if any) are unchanged, (2) continuum eigenvalues are rotated down in the complex energy plane by an angle 2θ, and (3) metastable complex eigenvalues (if any) are unchanged except that for sufficiently large angles of rotation they are now resident upon the first energy sheet, having been effectively "uncovered" due to effect (2) above (the continuum energies form the branch cut separating the two Riemann sheets). One then proceeds to solve the Schrödinger equation,

$$H_\theta \psi = (E_r - i \frac{\Gamma}{2}) \psi \quad , \tag{3.2}$$

by conventional bound state methods, i.e., by expanding the wavefunction ψ in a suitable basis set and diagonalizing the resulting complex symmetric matrix.

Recent work[18] on complex scaling has concluded that in a multi-dimensional problem it is actually not necessary to scale <u>all</u> coordinates but only the one associated with the dissociative degree of freedom. Furthermore, this is a desirable procedure to follow since the complex scale factor introduces oscillatory character into the basis functions, a correct feature for the dissociative degree of freedom but not so appropriate for the bound degrees of freedom.

Thus the scaled Hamiltonian for our model system has the form

$$H_\theta = - \frac{\hbar^2}{2m} e^{-2i\theta} \frac{d^2}{dx^2} - \frac{\hbar^2}{2m} \frac{d^2}{dy^2} + V(xe^{i\theta}, y) \quad , \tag{3.3}$$

where V is the potential energy function given by Eqs. (2.1) and (2.8). The wavefunction ψ is expanded as follows:

$$\psi = \sum_{n_x, n_y} C_{n_x, n_y} \phi_{n_x}(x) \chi_{n_y}(y) \quad , \tag{3.4}$$

where $\{\phi_{n_x}\}$ and $\{\chi_{n_y}\}$ are harmonic oscillator basis functions.

All matrix elements were computed using double precision word size so as to insure stability sufficient to obtain resonances with widths as small as 10^{-20}. In addition, all computations reported here used 40 basis functions for the x degree of freedom and 4 basis functions for the y degree of freedom. Truncation of the basis set expansion leads to slight dependence of the complex eigenvalues on the angle of rotation θ. Typically, regions of stability of angle trajectories are sought by graphical methods or complex Hellmann-Feynmann theorems,[17] but since the imaginary parts of eigenvalues were found to be stable to at least three significant figures (some to as many as 8) over at least 5 degrees of rotation, this procedure was unnecessary.

The results of these calculations are discussed below. The coupling parameters for the various systems are given in Table I.

System 1. (see Figure 2) This is the system with zero coupling as discussed in Section II. This is the extreme limit of mode-specific behavior.

Systems 2 and 3. (See Figures 3 and 4). These two systems illustrate the effects of the two types of coupling (frequency dilution for system 2, curvature for system 3) taken separately. It is clear from both systems that neither type of coupling alone results in significant statistical behavior. There is some tendency of the specific rates to coalesce along a single monotonically increasing

curve, but these systems are still highly mode-specific.

System 4. (see Figure 5). This system represents the combination of the two couplings, in the same strengths as for the systems 2 and 3 separately. It is obvious that their effects on the rates of decay are non-additive; i.e., their combined effect is to produce a system which is substantially more statistical than either of the two taken individually.

Systems 5, 6 and 7. (see Figures 6, 7 and 8). These systems illustrate the effects of intra-mode degeneracy upon the energy randomization process. Increased degeneracy between modes is expected to enhance the efficient energy transfer between modes,[5] thus resulting in greater randomization and "equal weighting" of all contributing states. System 6 represents the highest degree of degeneracy of the three systems, and along with the couplings present, leads to a strikingly statistical rate constant profile.

System 8. An interesting observation of these quantum mechanical systems is that there seems to be no energy requirement for statistical behavior in the unimolecular rate constant as there does for ergodic behavior in classical theory;[7] i.e., for these quantum systems statistical behavior is seen to occur at low energies to essentially the same extent that it occurs at higher energies, whereas classical ergodic behavior typically requires a threshold energy. This point is illustrated even more clearly by the final system, which was chosen to be one that exhibits a well-defined classical stochastic transition. Figure 9 shows, as before, the specific rates as a function of energy; the vertical dashed line at the lower energy indicates the on-set of

classical stochastic behavior (as seen in Poincare surfaces of section[7]), and the line at the higher energy indicates the top of the barrier. The specific rate constants show no more (or less) mode-specific character below the stochastic transition than they above it; i.e., mode-specificity in the rate constants seems to have little to do with the classical stochastic transition. The two are, of course, monitoring different phenomena. For the classical case the lifetime is infinite no matter what the energy of the particle (so long as it is below the top of the barrier); i.e., the system has an infinite amount of time to decide whether or not it is going to be ergodic. In considering unimolecular decay of the quantum system, on the other hand, even though the rate of unimolecular energy transfer increases with increasing energy so does the rate of unimolecular decomposition, so that the system has less time to randomize its internal energy before dissociation. It is thus not unreasonable for the degree of statistical behavior in the unimolecular rate constants, or conversely the degree of mode-specificity, to be similar for all energies, and for these quantum systems this is approximately the case.

IV. Semiclassical Model and Calculations

The quantum calculations of the previous section are the essentially exact results for the given model system, but such calculations would not be practical for real molecular systems, which have more than two degrees of freedom. There is thus interest in testing simpler approaches that, although less accurate, can be applied to more chemically interesting systems.

Classical trajectory simulations[19] can be readily carried out nowadays for small polyatomic molecules. If the total energy is above the classical barrier height for dissociation, it is thus possible to study unimolecular reactions with existing methodology.[5] We show here how a trajectory simulation can be combined with an approximate semiclassical treatment of tunneling in order to extend these capabilities to the energy region below the classical barrier height, as is the case for the present model of Section III (and also for the unimolecular decomposition of formaldehyde).

a. The Model

The basic physical idea of the approach is very simple: A classical trajectory is begun inside the potential well, and since the energy is below the barrier height it will oscillate in the well forever. Each time the trajectory hits the barrier (i.e., experiences of a classical turning point along the barrier direction), however, it is allowed to tunnel through it with a probability computed from the local properties of the trajectory at that time. The probability that by time t the particle has not tunneled out, i.e., the survival probability $P_s(t)$, is

$$P_s(t) = (1-P_1)(1-P_2) \ \ldots \ (1-P_{K(t)}) \quad . \tag{4.1}$$

where P_k is the tunneling probability for the k^{th} time the particle hits the barrier (or barriers if there is more than one decay channel, as for the potential well in Figure 1), and K(t) is the number of hits that have occurred by time t; Eq. (4.1) states that the net probability of not having tunneled out by time t is the probability of not tunneling out each time the particle hits the barrier.

Equation (4.1) gives the survival probability for a single trajectory, and this must be averaged over an appropriate distribution of trajectories (i.e., initial conditions); this is described in Section IVb. This averaged survival probability $\langle P_s(t) \rangle$ should decay exponentially, and the unimolecular rate constant k is obtained as the negative slope of a plot of $\ell n \langle P_s(t) \rangle$ versus t.

For small tunneling probabilities, i.e., $P_k << 1$, Eq. (4.1) is difficult to evaluate directly (because, for example, $1-10^{-14} \simeq 1$ on a computer), so it is useful to compute first the cummulative tunneling probability $P_{tun}(t)$,

$$P_{tun}(t) \equiv 1-P_s(t) \quad , \tag{4.2}$$

which can be shown to be given by

$$P_{tun}(t) = \sum_{k=1}^{K(t)} P_k(1-P_{k-1})(1-P_{k-2}) \ \ldots \ (1-P_2)(1-P_1) \quad ; \tag{4.3}$$

if $P_k << 1$, then Eq. (4.3) becomes

$$P_{tun}(t) = \sum_{k=1}^{K(t)} P_k \quad ,$$

and this causes no computational difficulty. This is averaged over initial condition as in Section IVb to give $\langle P_{tun}(t) \rangle$, and then the averaged survival probability is obtained by

$$\langle P_s(t) \rangle = 1 - \langle P_{tun}(t) \rangle \quad . \tag{4.4}$$

The key to the model is how the tunneling probabilities $\{P_k\}$ are computed. The most rigorous semiclassical approach would be to integrate the classical equations of motion along the complex time contours for which the particle tunnels through the barrier.[20] Approximate versions of this based on the assumption of vibrationally adiabatic motion through the barrier are much simpler to implement, and for the numerical results described below we have used the simplest such approximation, the vibrationally adiabatic zero curvature (VAZC) approximation.[21] Within this approximation the classical Hamiltonian used to describe the tunneling is

$$H(p_s,s,n) = \frac{p_s^2}{2m} + V_0(s) + (n+\tfrac{1}{2})\hbar\omega(s) \quad , \tag{4.5}$$

where s is the reaction coordinate (the steepest descent path down from the saddle point), n is the vibrational action variable (i.e., quantum number) for the transverse vibration, $V_0(s)$ is the potential energy along the reaction coordinate, and $\omega(s)$ is the transverse vibrational frequency as a function of the reaction coordinate. The classical trajectories themselves are computed using the full classical Hamiltonian

of Eq. (2.1); the approximate Hamiltonian in Eq. (4.5) is used only for the purpose of determining an approximate tunneling probability. At time t_k, the $k^{\underline{th}}$ turning point for motion along s, the current value of the vibrational action variable, n_k, is determined by energy conservation and Eq. (4.5):

$$n_k + \frac{1}{2} = \frac{E-V_0(s)}{\hbar\omega(s)}\Bigg|_{s=s(t_K)} \quad ; \tag{4.6}$$

the tunneling probability is then given within the VAZC approximation by

$$P_k = e^{-2\theta_k}/(1+e^{-2\theta_k}) \tag{4.7a}$$

where

$$\theta_k = \int_{s_<}^{s_>} ds\, \sqrt{2m[V_{eff}(s)-E]} \tag{4.7b}$$

$$V_{eff}(s) = V_0(s) + (n_k + \frac{1}{2})\hbar\omega(s) \quad . \tag{4.7c}$$

More accurate approximations to P_k are possible[13,22] even within the vibrationally adiabatic approximation, but they do not significantly alter the semiclassical results described below.

b. Initial Conditions

We wish to compute the survival probability, and thus the unimolecular rate constant, corresponding to a definite total energy E and a specific initial value for n_y, the zeroth order (i.e., harmonic), quantum number for the bound degree of freedom. Since n_y is only an

approximate quantum number for the coupled system, this type of mode-specific preparation of the system is not precisely equivalent to that produced by the quantum calculations of Section III if $V_c \neq 0$, but should be similar; in any event it does give the same kind of information, i.e., how the rate for a given total energy varies if the energy is initially distributed in the molecule in various ways.

To specify the average over initial conditions corresponding to a given E and initial n_y, one specifies the bound coordinate and momentum (y,p_y) in terms of their harmonic action angle variables,

$$y = \sqrt{\frac{(2n_y+1)\hbar}{m\omega_y}} \sin q_{n_y} \tag{4.8a}$$

$$p_y = \sqrt{(2n_y+1)\hbar m\omega_y} \cos q_{n_y} \quad ; \tag{4.8b}$$

n_y is set initially to an integer, the initial vibrational quantum number for the bound oscillator, and q_{n_y} is to be averaged over. In order to describe the methodology as it would be applied if there were many bound degrees of freedom, the average over q_{n_y} is carried out by Monte Carlo; i.e., q_{n_y} is chosen as $2\pi\xi_i$ for the i^{th} trajectory, where ξ_i is a random number. The x-motion is started always at a classical turning point; i.e., $p_x = 0$ and $x_<$ is then determined by energy conservation,

$$H(p_x,p_y,x,y) = E \quad . \tag{4.9}$$

The average over the phase of the x-motion is effected by averaging over time t for the first period of the x-oscillation. To see how this

is accomplished, consider the function $P_{tun}^{(i)}(t)$, the function $P_{tun}(t)$ of Eq. (4.3) for the i^{th} trajectory, i.e., the one with initial conditions

$$\begin{aligned} q_{n_y} &= 2\pi\xi_i \\ n_y &= \text{given integer} \\ p_x &= 0 \\ x &= x_< \text{ from Eq. (4.8)} \quad . \end{aligned} \tag{4.10}$$

$\{t_k^{(i)}\}$ and $\{P_k^{(i)}\}$, k=1,2, ..., denote the times of the x-turning points and the tunneling probabilities at these times, respectively; Figure 10 sketches the typical form of $P_{tun}^{(i)}(t)$. The explicit expression for $P_{tun}^{(i)}(t)$ is

$$P_{tun}^{(i)}(t) = \sum_{k=1}^{\infty} P_k^{(i)} \, h(t-t_k^{(i)}) \quad , \tag{4.11}$$

where the quantity $P_k^{(i)}$ is defined by

$$P_k^{(i)} = P_k^{(i)}(1-P_{k-1}^{(i)})(1-P_{k-2}^{(i)}) \ \ldots \ (1-P_2^{(i)})(1-P_1^{(i)}) \quad , \tag{4.12}$$

and h is the unit step function,

$$h(z) = \begin{cases} 1, & z > 0 \\ 0, & z < 0 \end{cases} \quad .$$

The time average and Monte Carlo average of Eq. (4.11) gives the desired averaged tunneling probability,

$$\langle P_{tun}(t)\rangle_{E,n_y} \equiv \frac{1}{N} \sum_{i=1}^{N} \frac{1}{t_1^{(i)}} \int_0^{t_1^{(i)}} dt' \; P_{tun}^{(i)}(t+t') \quad , \tag{4.13}$$

where N is the number of trajectories run, i.e., the number of Monte Carlo selections of q_{n_y}. The time average in Eq. (4.13) can be carried out explicitly by introducing the following function

$$Q_k^{(i)}(t) \equiv \frac{1}{t_1^{(i)}} \int_0^{t_1^{(i)}} dt' \; h(t+t'-t_k^{(i)}) \tag{4.14a}$$

$$= \left\{ \begin{array}{l} 0, \; t < t_k^{(i)} - t_1^{(i)} \\ 1 + (t-t_k^{(i)})/t_1^{(i)} \; , \; t_k^{(i)} - t_1^{(i)} < t < t_k^{(i)} \\ 1, \; t > t_k^{(i)} \end{array} \right\} \quad , \tag{4.14b}$$

so that the averaged tunneling probability is given finally by

$$\langle P_{tun}(t)\rangle_{E,n_y} = \frac{1}{N} \sum_{i=1}^{N} \sum_{k=1} P_k^{(i)} \; Q_k^{(i)}(t) \quad . \tag{4.15}$$

Equation (4.2) then gives the averaged survival probability,

$$\langle P_s(t)\rangle_{E,n_y} = 1 - \langle P_{tun}(t)\rangle_{E,n_y} \quad , \tag{4.16}$$

the exponential decay of which gives the rate constants $k_{n_y}(E)$.

When the total energy is above the top of the classical barrier height, the above equations reduce to the standard classical prescription

for computing the survival probability if the tunneling probabilities $\{P_k\}$ are set to 0 or 1 (depending on whether or not the classical motion passes over the barrier). In this case, for trajectory i one only needs to note the time $t_1^{(i)}$ that it passes over the barrier, and the above equations reduce to

$$1 - \langle P_s(t) \rangle_{E,n_y} = \frac{1}{N} \sum_{i=1}^{N} Q^{(i)}(t) \quad ,$$

where

$$Q^{(i)}(t) \equiv \frac{1}{t_1^{(i)}} \int_0^{t_1^{(i)}} dt' \; h(t+t'-t^{(i)})$$

$$= \begin{cases} 0, & t < t^{(i)} - t_1^{(i)} \\ 1 + (t-t^{(i)})/t_1^{(i)}, & t^{(i)} - t_1^{(i)} < t < t^{(i)} \\ 1, & t > t^{(i)} \end{cases} ;$$

$t_1^{(i)}$ is, as before, the time for the first oscillation in the x-potential well.

c. Results

Figure 11 shows a typical result for the exponential decay of the survival probability, from which the rate constant k is obtained. Calculations were carried out for all the cases studied quantum mechanically, and the agreement in general is reasonably good. For the separable case the VAZC approximation for the tunneling probability is essentially exact, and not surprisingly the semiclassical rate constants are in excellent agreement ($\sim$ 10% or better) with the quantum

results seen in Figure 2. Figure 12 shows the more typical comparison when there is coupling: The points are the quantum results for system 6 (Figure 7), which shows a high degree of statistical characater, and the solid curves are the semiclassical results as a continuous function of E (i.e., no attempt was made to quantize the x-mode semiclassically).

Thus even with the relatively primitive VAZC approximation for the tunneling probability, Eq. (4.7), the semiclassical model yields rates in reasonable qualitative agreement with the quantum values. It is certainly possible to employ more accurate approximations for determining the tunneling probabilities. These results are thus quite encouraging, for this semiclassical model can be applied with no more effort than required for a normal classical trajectory simulation without tunneling.

V. Concluding Remarks

Certain aspects of the results described in Section III are intuitively transparent: with no coupling between the modes the system is completely mode-specific, and coupling between them (and frequency matching as well) tends to destroy the mode-specificity. Real molecular systems may be expected to span the entire range of these possibilities; i.e., some molecules (e.g., Van der Waals complexes) will be extremely mode specific, whereas others will be highly statistical. To treat any particular case rigorously will thus require knowledge of the potential energy surface, although chemical empiricism (based on experimental and perhaps theoretical evidence) will undoubtedly lead to rules of thumb for correlating and predicting such behavior.

What was not anticipated in the results is the absence of any energy threshold for the onset of statistical character in the unimolecular rates. There thus seems to be no direct relation between statistical character of the unimolecular rates and stochastic character in the corresponding classical system. For example, Poincare surfaces of section for the classical systems corresponding to Figures 2-8 show no significant amount of stochastic behavior below the classical dissociation energy, whereas the unimolecular rate constants for some of these systems show a high degree of statistical behavior. Furthermore, the classical system corresponding to Figure 9 does show the onset of stochastic surfaces of section at a well-defined energy, but the statistical/mode-specific character of the unimolecular rate constants is essentially the same above and below this energy. We consider these observations to be important, although as with any study employing a

particular model it is not possible to say how general the conclusions are.

The semiclassical model described in Section IV is able to reproduce the exact quantum results of Section III reasonably well, and refinements of it--i.e., better approximations for the tunneling probability--are easily incorporated. This makes it possible to treat more physically realistic models, i.e., those with more than two degrees of freedom, within the framework of a classical trajectory simulation.

Finally, we note that in many cases the system is not prepared in one particular quasi-bound state. Consider, for example, the photodissociation of formaldehyde as in Eq. (1.3). For this case standard analysis[23] give the quantum mechanical survival probability as

$$P_s(t) = |S(t)|^2 \quad , \tag{5.1}$$

where

$$S(t) = \frac{1}{2\pi i} \int_{-\infty}^{\infty} dE \; \frac{e^{-iEt/\hbar}}{E-E_{s_1}-\Delta(E)} \tag{5.2}$$

$$\Delta(E) = \sum_n \frac{|\langle s_1|V|n\rangle|^2}{E-E_n + \frac{i\Gamma_n}{2}} \quad . \tag{5.3}$$

Here $|s_1\rangle$ and E_{s_1} denote the initial state, and its energy, of $H_2CO(S_1)^*$ that is excited by the photon; $|n\rangle$, E_n, and Γ_n are the quasi-bound vibrational states, and energy and width, in the ground electronic state S_0; and V is the electronically non-adiabatic coupling between S_1 and S_0. (If $\Delta(E)$ is set equal to $\Delta(E_{s_1})$ in the denominator of the

integrand in Eq. (5.2), then the integral is easily evaluated and gives

$$P_s(t) \propto e^{-kt}$$

$$k = \sum_n \frac{|\langle s_1|V|n\rangle|^2(\Gamma_n/\hbar)}{(E_{s_1}-E_n)^2 + (\Gamma_n/2)^2} \quad , \tag{5.4}$$

a well-known[24] approximation.) In this situation it is necessary to know the energies and lifetimes $\{E_n, \Gamma_n\}$ of the quasi-bound states of S_0, but this is not enough; one also needs to know the coupling between the initial state $|s_1\rangle$ and all the quasi-bound states $|n\rangle$.

Acknowledgments

This work has been supported in part by the Division of Chemical Sciences, Office of Basic Energy Sciences, U.S. Department of Energy under contract No. W-7405-Eng-48. All calculations were carried out on a Harris Slash Four minicomputer funded by a National Science Foundation Grant CHE-7622621.

Table I. Potential Parameters[a]

Figure	ω_x	ω_y	$\omega_y^{\ddagger}$[b]	η	V_2	$\hbar$	m
2	14.14	14.14	14.14	0.	0.	.5	1
3	14.14	14.14	7.27	2.0	0.	.5	1
4	14.14	14.14	14.14	0.	20.	.5	1
5	14.14	14.14	7.27	2.0	20.	.5	1
6	14.14	8.94	4.60	2.0	20.	.5	1
7	14.14	17.89	9.20	2.0	20.	.5	1
8	14.14	11.05	5.68	2.0	20.	.5	1
9	14.14	14.14	14.14	0	170.	.4	1

[a]For the potential function of Eq. (2.8) and the Hamiltonian of Eq. (3.3).

[b]The local frequency of the y-mode at the saddle point on the potential surface.

References

1. See, for example, (a) Advances in Laser Chemistry, ed. E. H. Zewail, Springer, N.Y., 1978; (b) Laser-Induced Processes in Molecules, ed. K. L. Kompa and S. D. Smith, Springer, N.Y., 1979.
2. R. E. Smalley, D. H. Levy, and L. Wharton, J. Chem. Phys. 64, 3266 (1976); M. S. Kim, R. E. Smalley, L. Wharton, and D. H. Levy, J. Chem. Phys. 65, 1216 (1976).
3. See, for example, I. Oref and B. S. Rabinovitch, Acct. Chem. Res. 12, 166 (1979).
4. (a) K. V. Reddy and M. J. Berry, Chem. Phys. Lett. 66, 223 (1979); (b) R. Naaman, D. M. Lubman, and R. N. Zare, J. Chem. Phys. 71, 4192 (1979); (c) R. B. Hall and A. Kaldor, J. Chem. Phys. 70, 4027 (1979).
5. See, for example, (a) S. A. Rice, ref. 1a, p. 2; (b) R. A. Marcus, D. W. Noid, and M. L. Koszykowski, ref. 1a, p. 298; (c) S. Nordholm and S. A. Rice, J. Chem. Phys. 61, 203, 768 (1974); (d) D. W. Oxtoby and S. A. Rice, J. Chem. Phys. 65, 1676 (1976); (e) R. M. Stratt, N. C. Handy, and W. H. Miller, J. Chem. Phys. 71, 3311 (1980); (f) K. G. Kay, J. Chem. Phys. 61, 5205 (1974); (g) C. S. Sloane and W. L. Hase, J. Chem. Phys. 64, 2256 (1976); (h) S. B. Woodruff and D. L. Thompson, J. Chem. Phys. 71, 376 (1979); (i) Stochastic Behavior in Classical and Quantum Hamiltonian Systems, ed. J. Ehlers, K. Hepp, R. Kippenhahn, H. A. Weidenmüller, and J. Zittartz, Springer, N.Y., 1979.
6. For example, see (a) D. L. Bunker, J. Chem. Phys. 37, 393 (1962); 40, 1946 (1964); (b) E. Thiele and D. J. Wilson, J. Chem. Phys. 35, 1256 (1961); 38, 1959 (1963).

7. For a review, see J. Ford, Adv. Chem. Phys. 24, 155 (1973).

8. See, for example, (a) E. S. Yeung and C. B. Moore, J. Chem. Phys. 58, 3988 (1973); (b) R. G. Miller and E. K. C. Lee, J. Chem. Phys. 68, 4448 (1978) and references therein.

9. See, for example, (a) P. J. Robinson and K. A. Holbrook, Unimolecular Reactions, Wiley, 1972; (b) W. Forst, Theory of Unimolecular Reactions, Academic Press, 1973.

10. See, for example, W. H. Miller, Adv. Chem. Phys. 30, 77 (1975).

11. W. H. Miller, J. Am. Chem. Soc. 101, 6810 (1979).

12. B. Barbanis, Astron. J. 69, 73 (1964).

13. See, for example, (a) R. A. Marcus, J. Chem. Phys. 45, 4493, 4500 (1966); 49, 2610 (1968); (b) W. H. Miller, N. C. Handy, and J. E. Adams, J. Chem. Phys. 72, 99 (1980).

14. See, for example, T.-Y. Wu and T. Ohmura, Quantum Theory of Scattering, Prentice-Hall, 1962.

15. A. J. F. Siegert, Phys. Rev. 56, 750 (1939).

16. See also (a) J. N. Bardsley and B. R. Junker, J. Phys. B. 5, L178 (1972); R. A. Bain, J. N. Bardsley, B. R. Junker, and C. V. Sukumar, J. Phys. B 7, 2189 (1974); (c) A. D. Isaacson, C. W. McCurdy, and W. H. Miller, Chem. Phys. 34, 311 (1978).

17. See, for example, Int. J. Quant. Chem. 14, No. 4 (October) 1978, the entire volume of which is devoted to complex scaling.

18. (a) T. N. Rescigno, C. W. McCurdy and A. E. Orel, Phys. Rev. A 17, 1931 (1978); (b) B. R. Junker and C. L. Huang, Phys. Rev. A 18, 313 (1978).

19. See, for example, R. N. Porter and L. M. Raff, in Dynamics of Molecular Collisions Part B (Vol. 2 of Modern Theoretical Chemistry),

ed. W. H. Miller, Plenum, N.Y., 1976, p. 1; W. H. Hase, ibid, p. 121.

20. W. H. Miller, Adv. Chem. Phys. 25, 69 (1974).

21. (a) R. A. Marcus, J. Chem. Phys. 46, 959 (1967); (b) R. E. Wyatt, J. Chem. Phys. 51, 3489 (1969); (c) D. G. Truhlar, J. Chem. Phys. 53, 2041 (1976).

22. R. A. Marcus and M. E. Coltin, J. Chem. Phys. 67, 2609 (1977).

23. M. L. Goldberger and K. M. Watson, Collision Theory, Wiley, N.Y., 1964, p. 424, et seq.

24. (a) B. Sharf and R. Silbey, J. Chem. Phys. 53, 2626 (1970); (b) A. Nitzan and J. Jortner, Theoret. Chim. Acta 29, 97 (1973); see also (c) G. D. Gillispie and E. C. Lim, Chem. Phys. Lett. 70, 532 (1980).

Figure Captions

1. Sketch of the potential well $V_1(x)$ for the dissociative degree of freedom; the functional form is given by Eq. (2.8a).

2. Rate constants, $k \equiv \Gamma/\hbar$, for unimolecular decay versus total energy E, for the quasi-bound states of the two-oscillator system. This case is for no coupling between the two modes.

3-8. Sames as Figure 2, except for the potential parameters as given in Table I.

9. Same as Figure 2, except for the potential parameters as given in Table I. The vertical lines indicate the energies at which classical stochastic trajectories first become significant (lower energy) and the top of the classical barrier.

10. Sketch of the cumulative tunneling probability for a given trajectory; i.e., a given set of initial conditions. $\{t_k\}$ indicates the times at which the trajectory hits the barrier, and $\{P_k\}$ is the tunneling probability for this "hit". See Section IVa.

11. Typical exponential decay of the averaged survival probability $\langle P_s(t)\rangle_{E,n_y}$, defined by Eq. (4.12)-(4.16), for the semiclassical model of Section IV.

12. Rate constants as a function of total energy, for the same system as in Figure 7. The points are the quantum mechanical values (the same as in Figure 7), and the curves are the semiclassical rates $k_{n_y}(E)$ obtained from the exponential decay of the survival probability $\langle P_s(t)\rangle_{E,n_y}$.

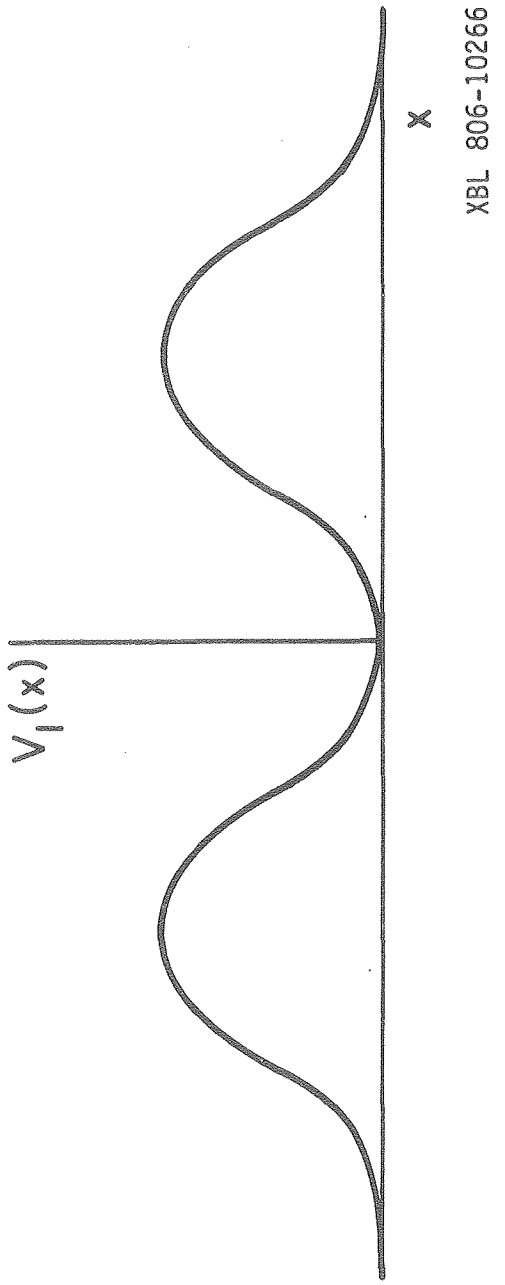

Figure 1

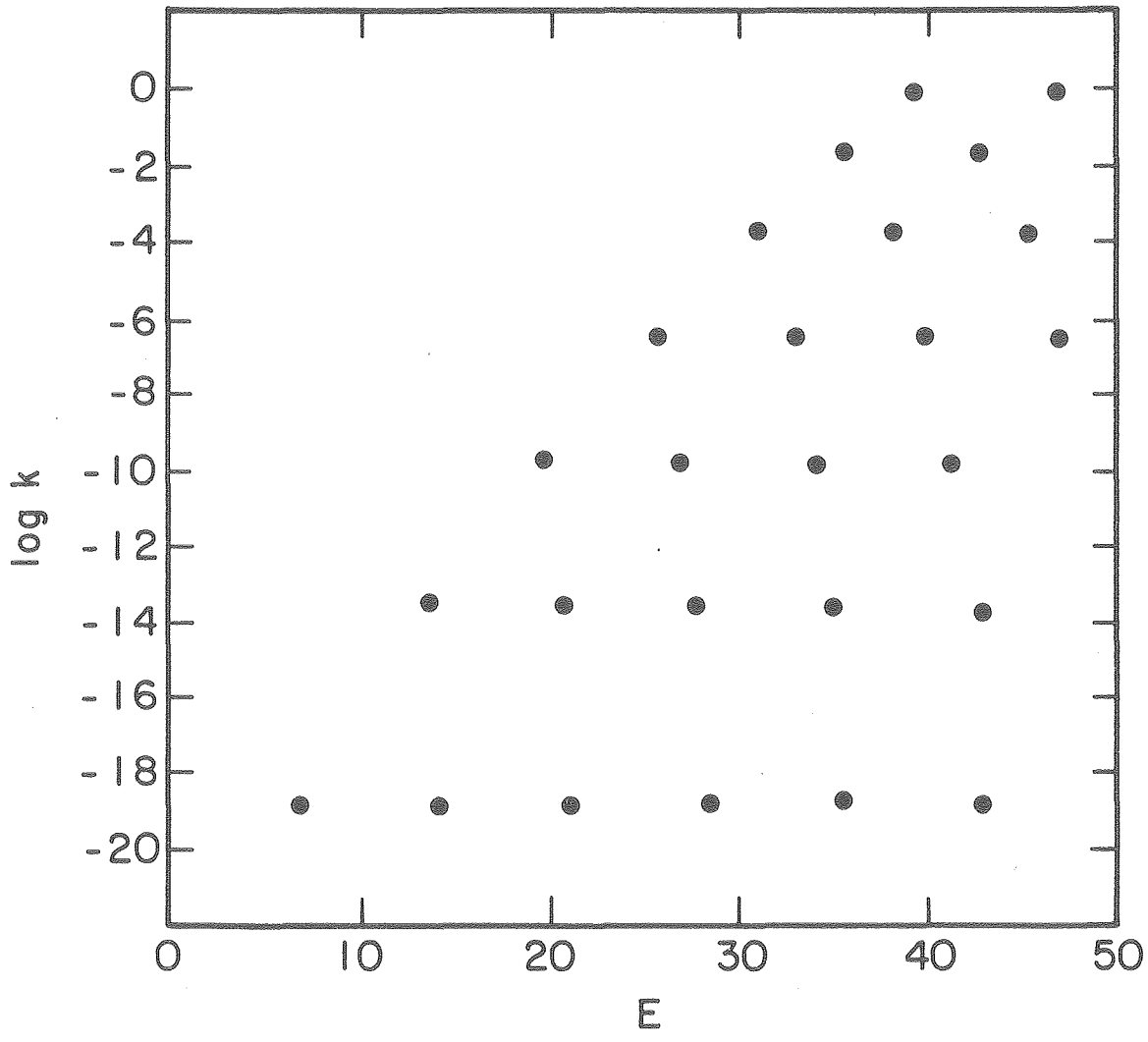

Figure 2

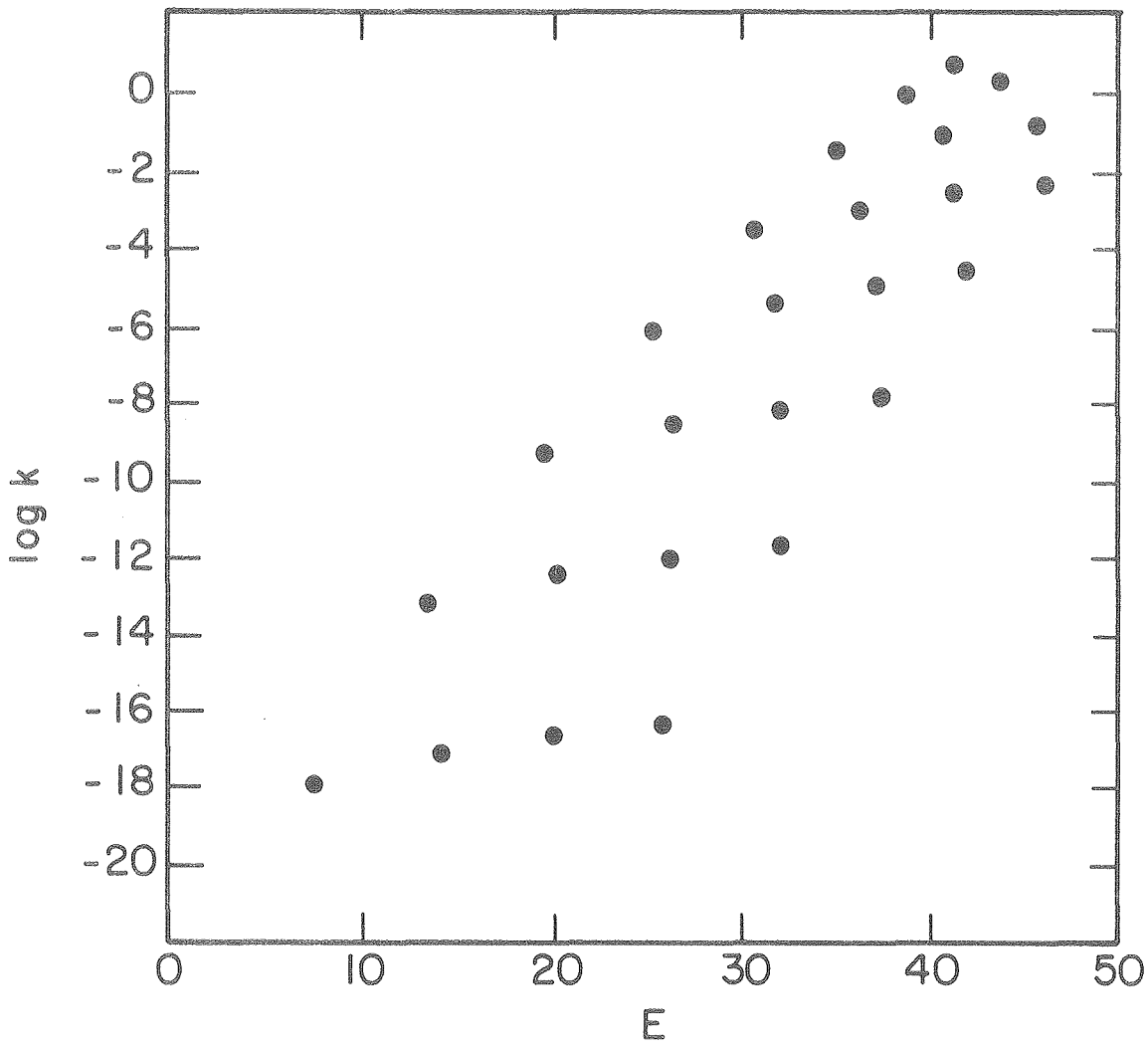

XBL 806-10268

Figure 3

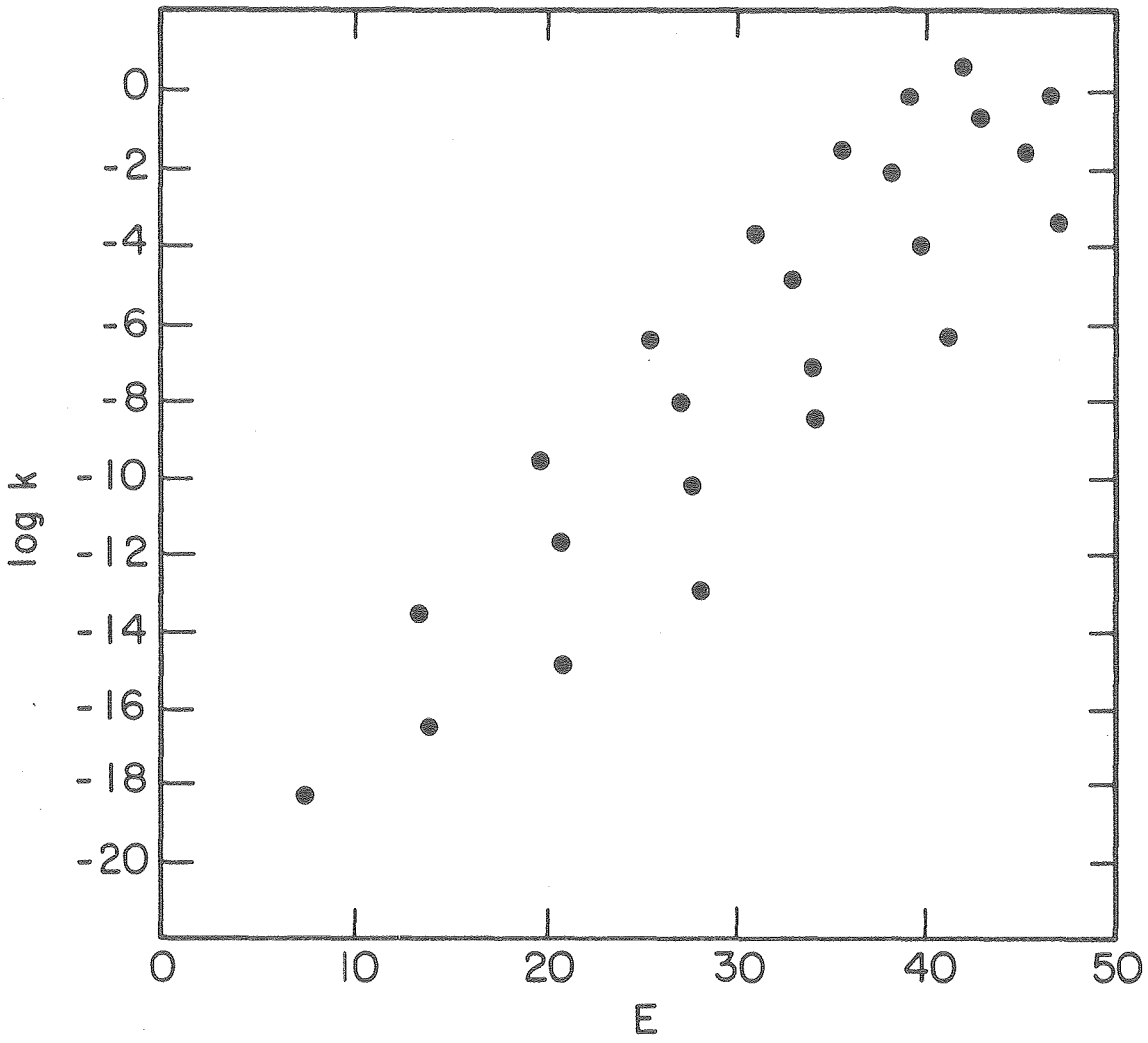

XBL 806-10269

Figure 4

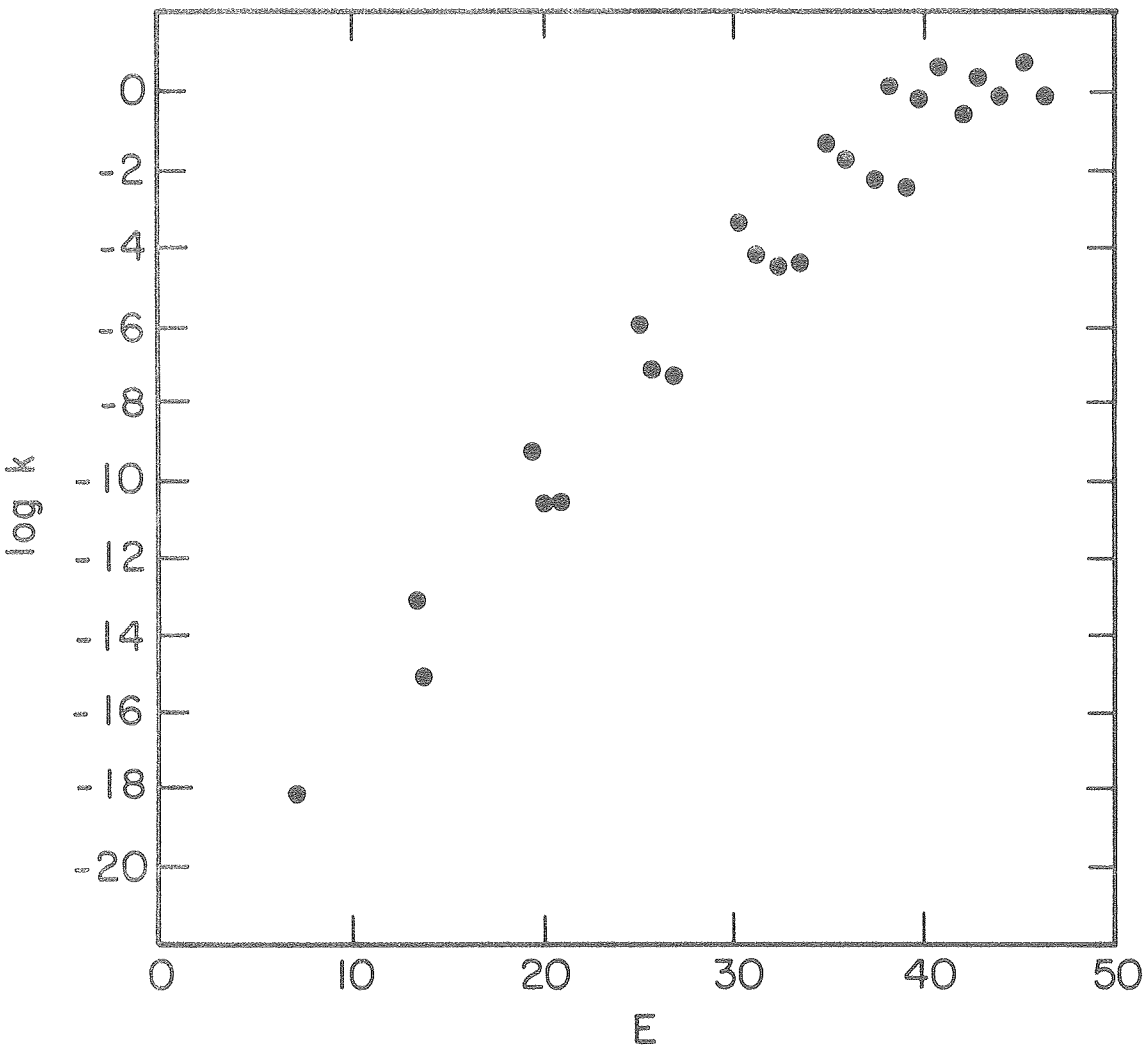

Figure 5

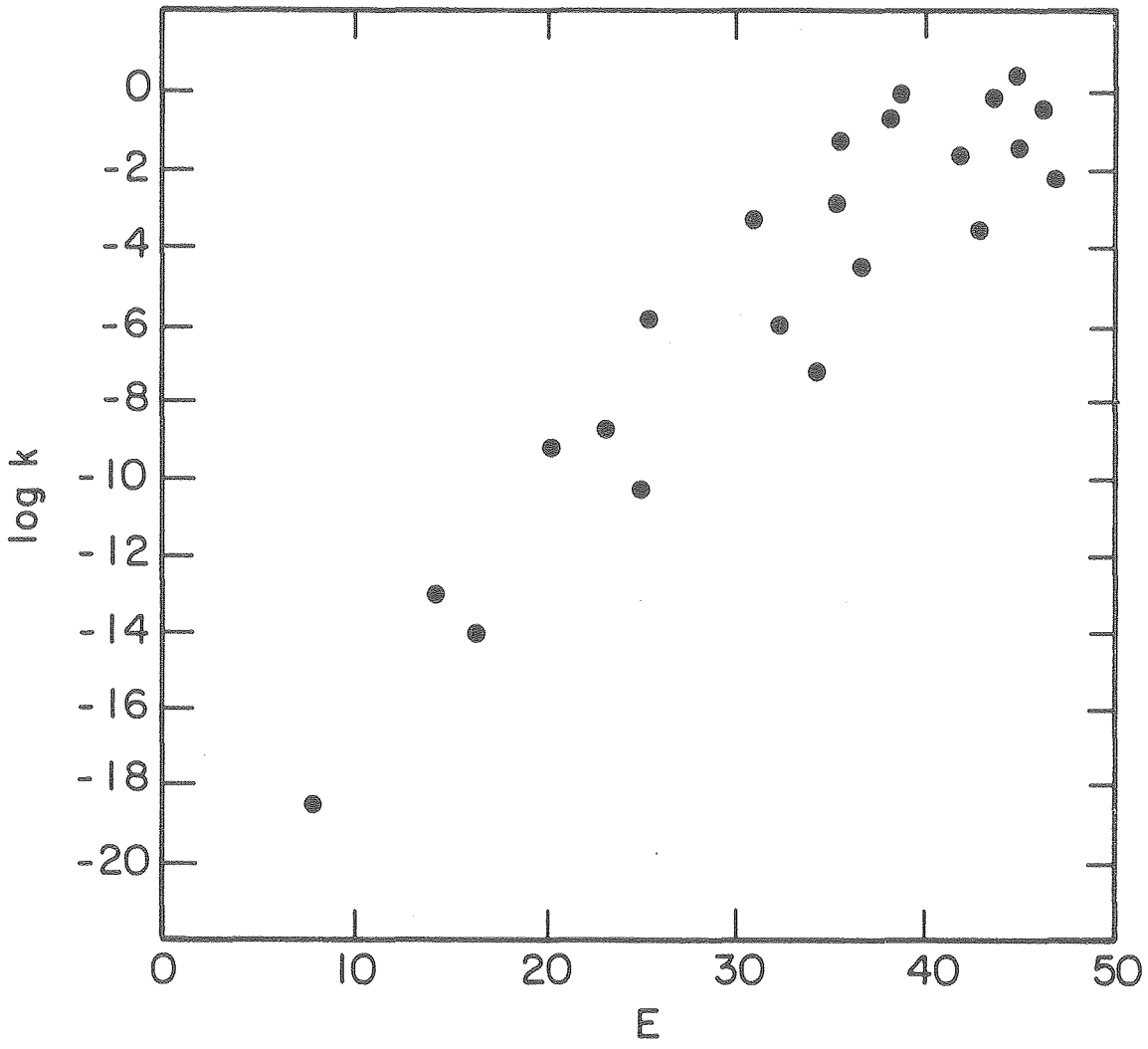

Figure 6

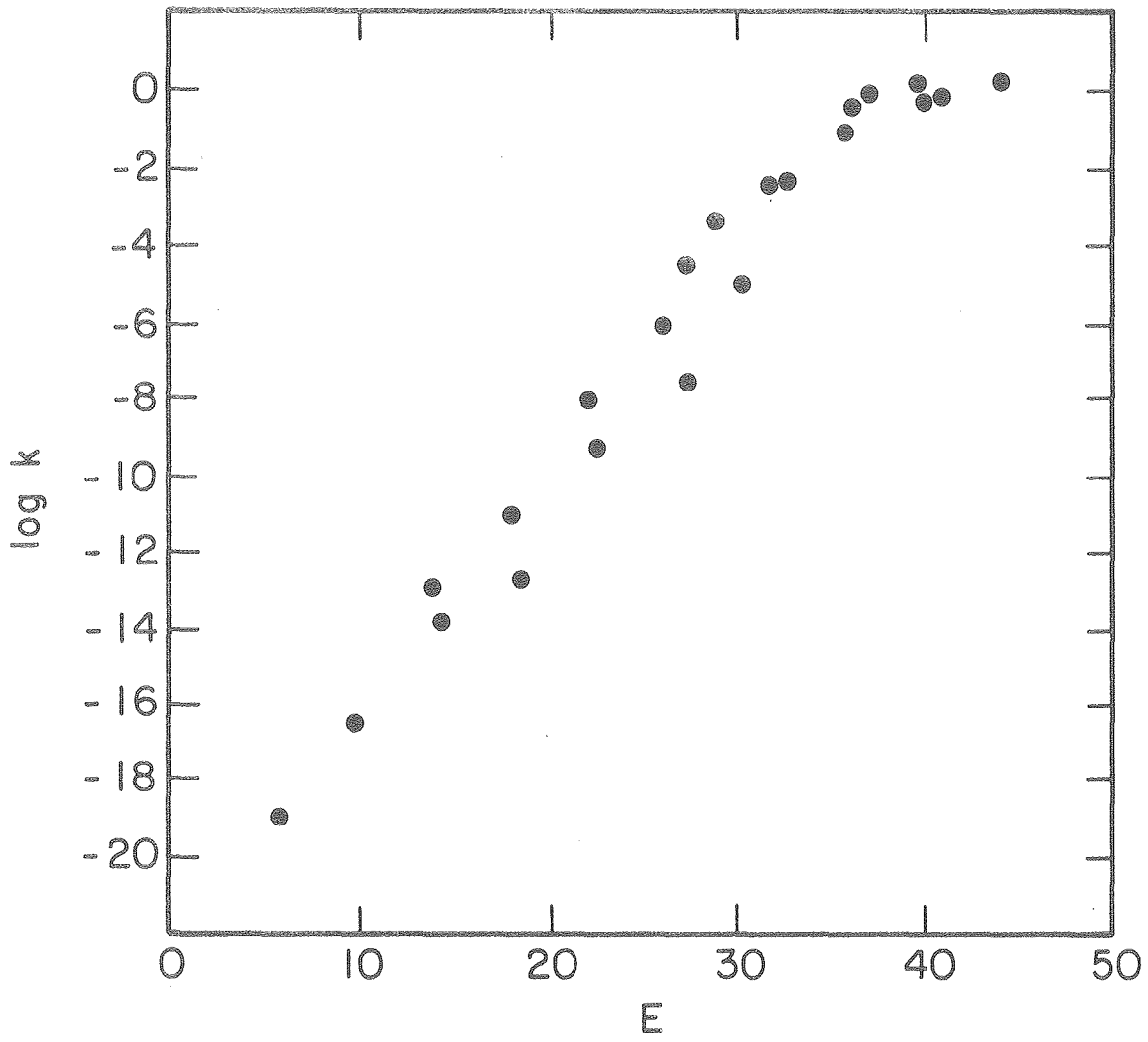

XBL 806-10272

Figure 7

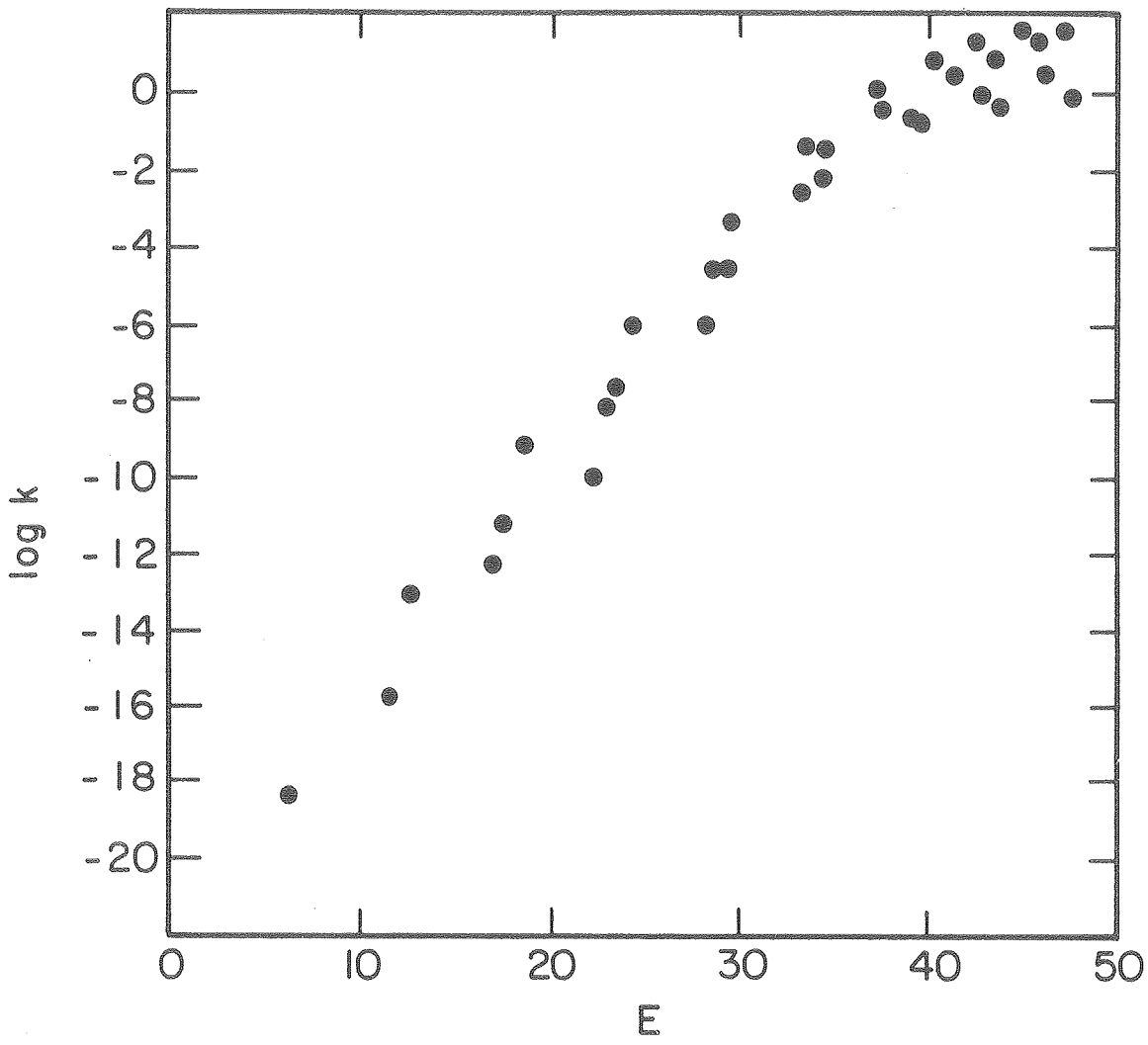

XBL 806-10273

Figure 8

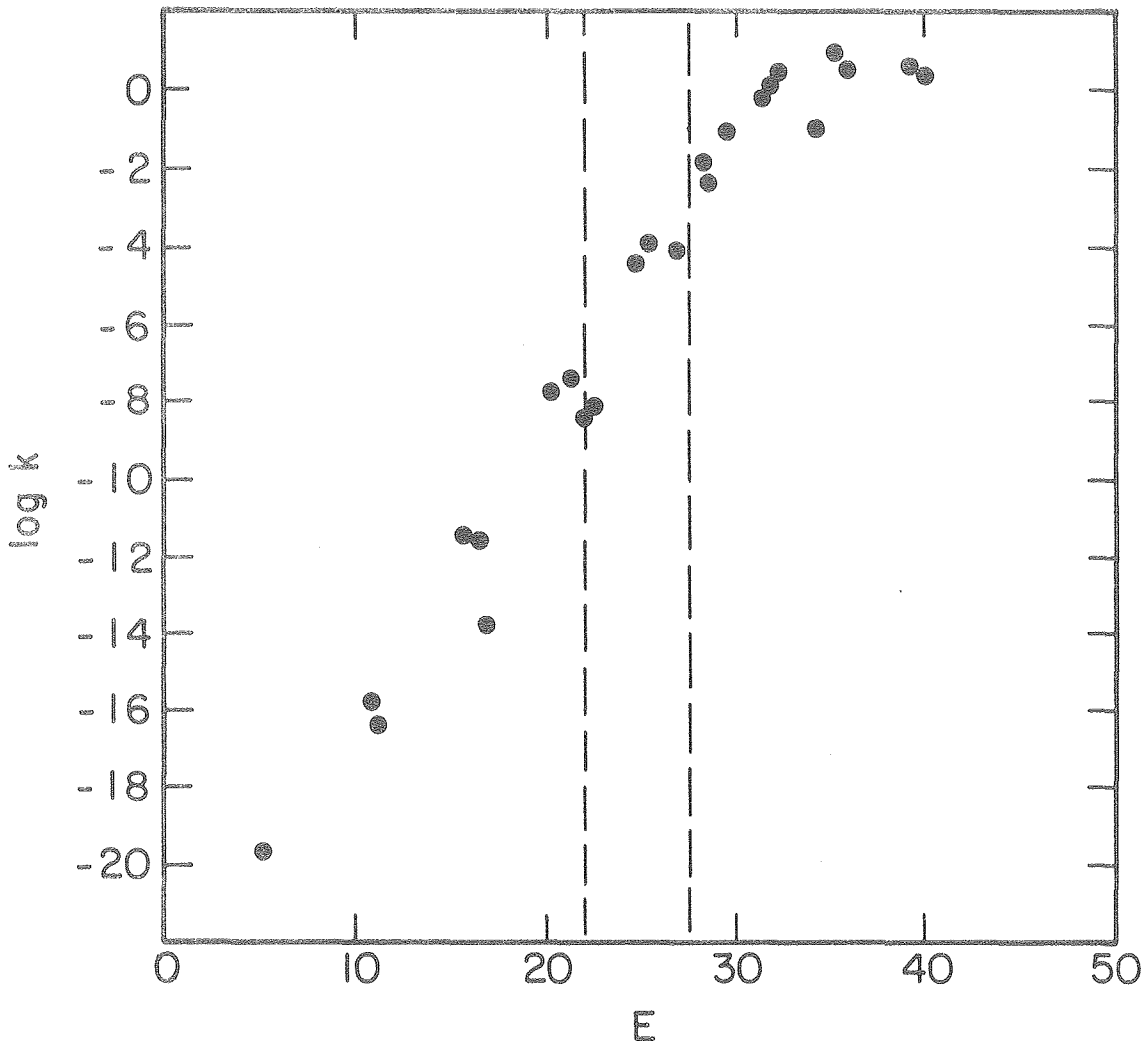

XBL 806-10274

Figure 9

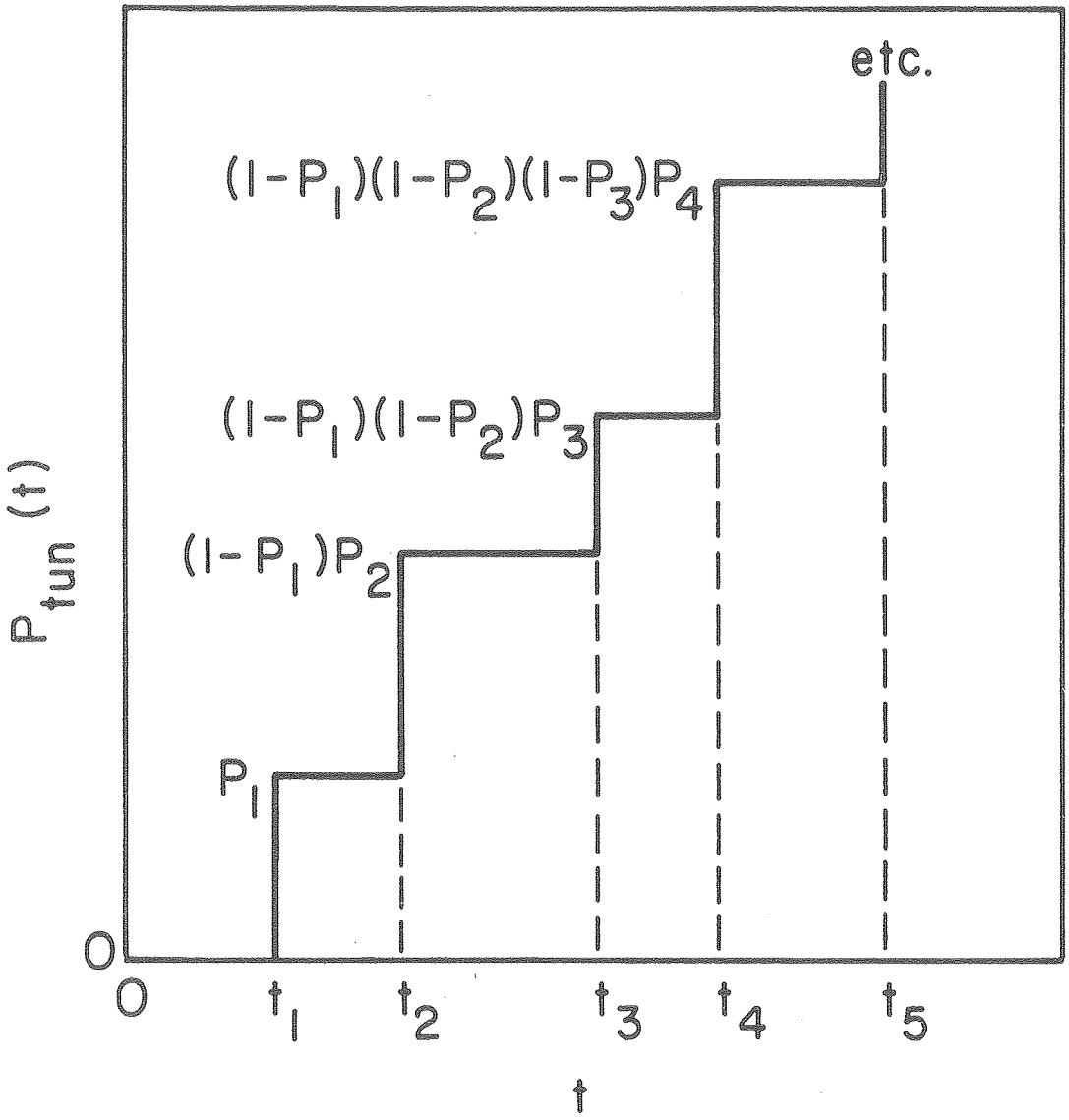

XBL 806-10275

Figure 10

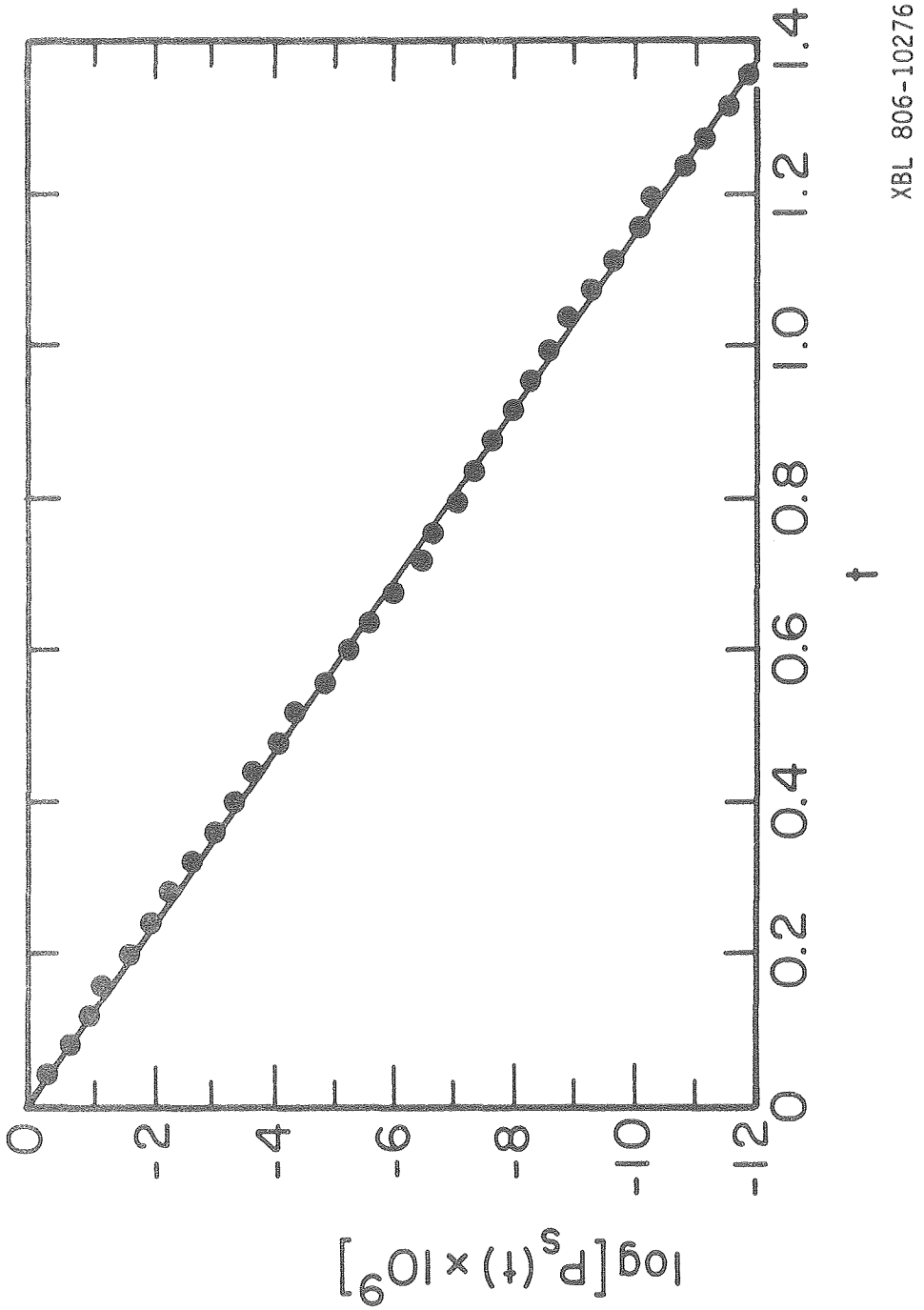

Figure 11

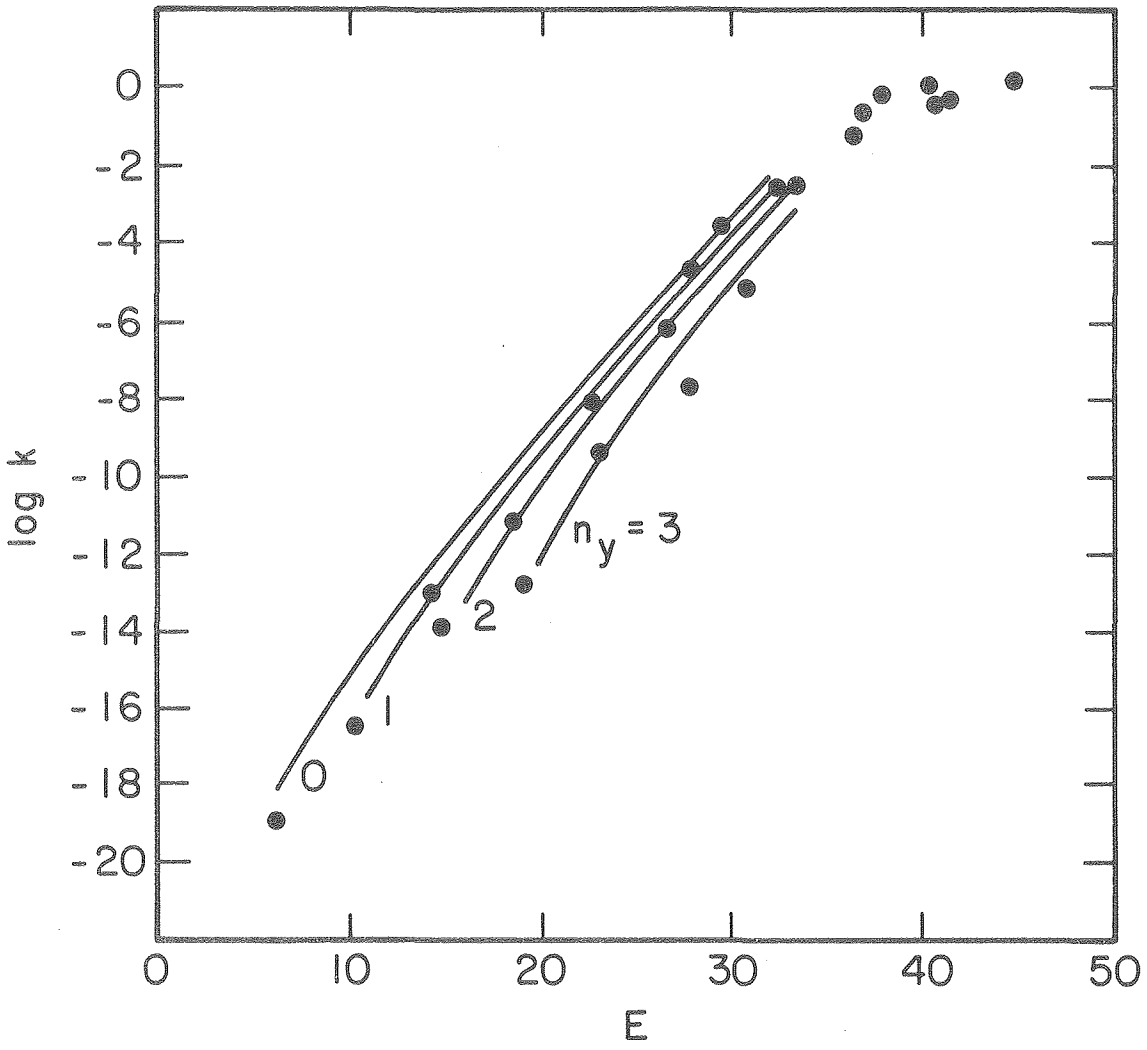

XBL 806-10277

Figure 12